

Coster-Kronig yields in silver measured with synchrotron radiation

Stacey L. Sorensen

Department of Physics and Chemical Physics Institute, University of Oregon, Eugene, Oregon 97403

Roger Carr

Stanford Synchrotron Radiation Laboratory, Stanford, California 94305

Stephen J. Schaphorst, Scott B. Whitfield, and Bernd Crasemann

Department of Physics and Chemical Physics Institute, University of Oregon, Eugene, Oregon 97403

(Received 30 January 1989)

The Coster-Kronig transition probabilities f_{ij} for shifting a vacancy from the L_i to the L_j subshell of Ag have been measured by differential photoionization of the subshells with synchrotron radiation by observing the intensity of the ensuing L_j - $M_{4,5}$ $M_{4,5}$ Auger transitions. In the course of the analysis, spectator satellites in these Auger spectra were identified. The following Ag Coster-Kronig yields were determined: $f_{23}=0.16\pm 0.03$, $f_{12}=0.044\pm 0.004$, and $f_{13}=0.61\pm 0.05$. While f_{23} agrees very well with relativistic independent-particle calculations by Chen *et al.* [Phys. Rev. A **24**, 117 (1981)], f_{12} and f_{13} fall below predictions by 35% and 18%, respectively, in qualitative accord with expected many-body effects.

I. INTRODUCTION

The radiationless transfer of vacancies among atomic subshells with the same principal quantum number constitutes a peculiar class of Auger processes named after its discoverers, Coster and Kronig.¹ Large wave-function overlap in their matrix elements causes Coster-Kronig transitions to be the fastest known to occur in atoms; they can cause hole-state widths of tens of electron volts² and tend to dominate the characteristics of the vacancy cascades through which atoms deexcite following inner-shell ionization.³

Calculations of Coster-Kronig rates are challenging. The intensity of these transitions taxes the limits of perturbative approaches. Many-body effects are pronounced; standard independent-particle calculations can lead to transition probabilities that exceed measurements by large factors, and even inclusion of the effects of exchange, electron correlation, and relaxation falls short of fully accounting for the physical situation.⁴ Interaction with the continuum affects the rates⁵ and the pertinent level energies.⁶ The extreme energy sensitivity of the rates calls for energy calculations that include the effects of relativity and quantum electrodynamics,⁷ as well as static and dynamic correlations.⁸ The need for experimental information to guide theoretical efforts is therefore pronounced.

Coster-Kronig electron spectra are difficult to measure because of their low energy; they have been determined in only a few cases.⁹ More amenable to measurement are bulk quantities known as Coster-Kronig yields, denoted by f_{ij}^X , which represent the total probability that a vacancy in the subshell i of the atomic shell X "bubbles up" to subshell j of the same shell, through any channel.³ Measurements of Coster-Kronig yields have been performed in which direct photoexcitation or radioactive decay pro-

vides the initial vacancies, while high-resolution spectroscopic techniques are used for analysis of photons and emitted electrons.³ The creation of an initial vacancy can be signalled by an Auger electron or photoelectron, x-ray or nuclear radiation. Coincident detection of a second decay product from a transition to a higher subshell indicates that vacancy transfer has taken place. In particular, coincidences between $K\alpha$ and L x rays have been used successfully to determine Coster-Kronig yields for some of the heavier elements,^{10,11} but are difficult to apply for low- and medium- Z species and cannot be used for the L_1 subshell, the $1s$ - $2s$ radiative transition being electric-dipole-forbidden. Information on Coster-Kronig rates can also be extracted from the intensities of satellites produced in transitions that follow Coster-Kronig decay, since the atom is left in a doubly ionized state. Only fragmentary information has, however, been accumulated by all these methods.

A promising new method for the determination of Coster-Kronig yields has become possible with the availability of tunable synchrotron radiation. This approach, first applied by Jitschin and collaborators,¹²⁻¹⁴ is based on selective ionization of subshells and detection of subsequent radiation. Here we describe a pilot experiment in which Ag L -shell Coster-Kronig yields were measured by ionizing the L subshells selectively while the photon-excited $L_{2,3}$ - $M_{4,5}$ $M_{4,5}$ Auger spectrum was monitored.

II. EXPERIMENT AND ANALYSIS

A. Apparatus

The experiment was performed with synchrotron radiation from the SPEAR electron storage ring in the Stanford Synchrotron Radiation Laboratory. X rays in the energy range from 3380 to 3850 eV were selected by two

Ge(111) Bragg reflections in the JUMBO double-crystal monochromator.

The Ag sample was evaporated *in situ* in the target chamber onto an Al substrate to a thickness of 15 monolayers at a base pressure of 10^{-6} Torr. The thickness of the deposited metal was gauged by comparison with test evaporations performed with a crystal thickness monitor in which the deposited mass can be deduced from the frequency of vibration of the substrate. During irradiation the sample chamber was open to the ring vacuum; its background pressure was kept below 10^{-9} Torr.

The incident photon flux was monitored by measuring the photoelectron yield from a gold grid (40 lines/cm, 90% transmission) placed in the beam path at the entrance to the sample chamber. The current from an electron multiplier facing the grid was recorded and averaged over each scan. Auger and photoelectron spectra were measured with a Physical Electronics Model 15-255 double-pass cylindrical-mirror analyzer in the retarding pulse-counting mode, operated at 100-eV pass energy. The x-ray monochromator setting, analyzer retarding potential, data collection, and storage were computer controlled.

B. Method

The experimental method employed here is based on the capability of selectively ionizing the subshells of sample atoms by means of highly monochromatic synchrotron radiation.¹²⁻¹⁴ The number of vacancies produced in each subshell can be determined to good accuracy from the theoretical photoionization cross sections of Scofield¹⁵ and knowledge of the incident x-ray energy and flux.

Scofield's subshell photoionization cross-section computation¹⁵ includes all contributing multipoles as well as retardation effects in the treatment of the radiation field. The electron wave functions are relativistic. Despite the fact that a Hartree-Slater (local-approximation) central potential for free atoms is employed and the same potential is used for the initial and final states, the results are very accurate.¹⁶ Careful experimental tests performed on elements 72-82 indicate agreement between theoretical and measured *L*-subshell cross sections to better than $\pm 2\%$.¹⁷ Photon energies employed in the present experiment are sufficiently well removed from absorption edges so that extended x-ray-absorption fine-structure (EXAFS) effects do not influence the cross sections significantly; multielectron effects in the form of shake processes are taken into account as discussed below. Energy interpolation between listed¹⁵ subshell photoionization cross sections was performed by means of an orthonormal routine.

The x-ray energy is determined by the angle of the two Bragg reflections from the Ge(111) crystals in the JUMBO monochromator. The energy scale was established by scanning the photon energy across the sulfur K edge at 2472 eV. The accuracy of the energy calibration is estimated to be better than ± 0.5 eV. The full width at half maximum of the synchrotron radiation of this energy scattered from the Ge(111) crystal was measured by Husains *et al.*¹⁸ to be 1.8 eV. The flux of photons from the

monochromator at 3 keV is $\sim 10^{11}$ photons/sec for a storage-ring current of 50 mA of 3-GeV electrons. The total photoelectron-yield cross sections at pertinent x-ray energies, required to interpret the electron current from the beam-flux monitoring Au grid, was calculated according to the algorithm of Berger and Hubbell,¹⁹ which is based on Scofield's¹⁵ cross sections.

The principle of the method for determining Coster-Kronig yields f_{ij} can be illustrated with reference to Fig. 1. X rays of energy E_3 are employed to ionize the L_3 subshell. The most intense Auger spectrum arising from L_3 -shell ionization, viz., that of the $L_3-M_{4,5}M_{4,5}$ transitions, is measured; let the relative intensity of these Auger electrons be $N_{A3}(E_3)$. If the x-ray energy is now increased to E_2 (Fig. 1), the L_2 subshell is ionized as well, and the new Auger counting rate $N_{A3}(E_2)$, normalized for identical incident-photon flux, will be proportional to the number of primary vacancies created by photoionization of the L_3 subshell at this x-ray energy plus the number of vacancies created in the L_2 subshell that are transferred to the L_3 subshell with probability f_{23} .

Denoting the photoionization cross section of the L_i subshell for photon energy E_j by $\sigma_i(E_j)$, it can then readily be shown that the L_2 - L_3 Coster-Kronig yield f_{23} is

$$f_{2,3} = \left[\frac{N_{A3}(E_3)\sigma_3(E_3)}{N_{A3}(E_3)\sigma_3(E_2)} - 1 \right] \frac{\sigma_3(E_2)}{\sigma_2(E_2)}. \quad (1)$$

Similarly, for incident x rays of energy E_1 (Fig. 1), the number of resultant L_3 vacancies will be the sum of those produced by direct L_3 ionization, those produced by L_2 ionization and transferred with probability f_{23} , and those produced by L_1 ionization and transferred with probability $(f_{13} + f_{12}f_{23})$. The ratio of measured L_3 Auger-electron intensities under excitation with x rays of energies E_1 and E_3 , for equal photon flux, can then be expressed as follows as a function of f_{12} , f_{13} , f_{23} , and of

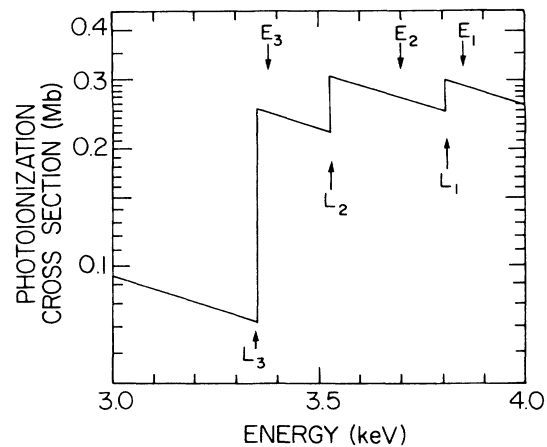


FIG. 1. Photoionization cross section of Ag in the *L*-shell region, as a function of x-ray energy, with indication of the photon energies E_i at which the present experiment was performed.

the pertinent subshell photoionization cross sections:

$$f_{1,3} = \frac{N_{A3}(E_1)\sigma_3(E_2)}{N_{A3}(E_3)\sigma_2(E_2)} - \frac{\sigma_3(E_1)}{\sigma_1(E_1)} - \left[\frac{\sigma_2(E_1)}{\sigma_1(E_1)} + f_{1,2} \right] f_{2,3} . \quad (2)$$

Finally, the Coster-Kronig yield f_{12} can be determined by measuring the ratio of a suitable L_2 Auger intensity, such as L_2 - $M_{4,5}M_{4,5}$, under excitation with x-ray energies E_1 and E_2 :

$$f_{1,2} = \left[\frac{N_{A2}(E_1)\sigma_2(E_2)}{N_{A2}(E_2)\sigma_2(E_1)} - 1 \right] \frac{\sigma_2(E_1)}{\sigma_1(E_1)} . \quad (3)$$

C. Auger spectra, satellites, and solid-state shifts

The energies of the main lines in the L - MM Auger spectra were based on the work of Mariot *et al.*,²⁰ who performed a systematic study of the Ag L_3 - $M_{4,5}M_{4,5}$ Auger energies and relative multiplet component intensities (Table I). Additional peaks are seen to be excited in the Auger multiplet group as the incident photon energy is increased. These can be ascribed primarily to satellite Auger lines which arise when spectator vacancies are created in an atom prior to Auger decay. The identification of the satellites which appear in the spectra was made by calculating their energies. For this purpose it is necessary to know multiple-vacancy energies and the corresponding atom-solid-energy shifts. We followed the approach of Ohno and Wendin,²¹ who have developed a simple approximation scheme to calculate these quantities in terms of the screened hole-hole repulsion, based on the knowledge of single-hole relaxation shifts and of the bare hole-hole Coulomb repulsion from the no-hole ground-state configuration.

The Auger energy of an electron emitted in a j - kl transition in a solid is written

$$E_{j-kl} = \sum_{x=j}^l E_x - \frac{1}{2} \sum_{x,y=j}^l \bar{F}^0(x,y) . \quad (4)$$

Here, E_x is defined as the single, relaxed-hole energy, and $\bar{F}^0(x,y)$ is the screened Coulomb interaction of holes in the x and y levels of the atom. The effect of N holes in the j th shell on the level energy then is

$$E_j(j^N) = E_j - N\bar{F}^0(j,j) . \quad (5)$$

Atom-solid-energy shifts are based upon the bare hole-hole Coulomb repulsion from the no-hole ground-state configuration and from single-hole relaxation shifts from photoelectron energies. The shifts include the screened hole-hole repulsion of the atomic final state.

The core-hole energy is estimated as

$$E_i^a = E_i^0 + \Delta_i^{ma} + \Delta_i^c , \quad (6a)$$

$$E_i^s = E_i^a + \Delta_i . \quad (6b)$$

Here, E_i^a is the energy of the core hole in a free atom, and E_i^s that energy if the atom is in a solid. The Hartree-Fock ground-state eigenvalue is E_i^0 , Δ_i^{ma} is the atomic monopole relaxation shift, and Δ_i^c is the ground-state correlation shift. The atom-solid shift Δ_i is the sum of three terms: the chemical shift, the energy shift due to configuration change in going from free atom to solid, and an extra-atomic relaxation shift.

The atom-solid energy shift in the i - jk Auger-electron energy then is

$$\delta\epsilon_{i-jk} = \Delta_j + \Delta_k - \Delta_i - \delta I_{jk} , \quad (7)$$

i.e., the sum of the atom-solid-energy shifts of the two final-state holes minus that of the initial core hole, minus the change in the Auger parameter δI_{jk} , which describes the atom-solid change of the effective Coulomb interaction between the holes j and k , viz., the change in screening between the atom and the solid. Ohno and Wendin²¹ point out that the change in Auger parameter is due primarily to extra-atomic relaxation and depends only weakly on chemical and configuration changes. For core holes, the Auger energy shift becomes level independent and takes on a particularly simple approximate form, viz.,

$$\delta\epsilon_{i-jk} \cong \Delta - \delta I_{jk} . \quad (8)$$

For a state with N holes between which no distinction is made, we have for the atom-solid energy shift

$$\Delta_{jN} \cong N[\Delta_j + (N-1)\Delta_j^{\text{ext}}] . \quad (9)$$

The extra-atomic relaxation shifts Δ_j^{ext} and single-hole atom-solid-energy shifts Δ_j for several elements have been determined by various authors through experimental and semiempirical methods based on the shifts between vapor-state and solid-state photoelectron and Auger energies.²¹

In order to interpret the Auger spectra measured in the present work, satellite energies were computed by first calculating the free-atom multihole transition energies through the change in self-consistent-field (Δ SCF) method with Hartree-Fock wave functions from the code of Froese-Fischer.²² The atom-solid shifts, found from the linear-response approximation of Ohno and Wendin²¹ described above, were then combined with the Δ SCF energies. Results for the most intense satellites are listed in Table II.

A satellite which appears ~ 5 eV below the 1G_4 diagram line in both the L_2 - and L_3 - $M_{4,5}M_{4,5}$ spectra,

TABLE I. Relative Ag L_3 - $M_{4,5}M_{4,5}$ Auger multiplet energies (from Mariot *et al.*, Ref. 20) and calculated intensities.

Multiplet component	Energy (eV)	Intensity (relative)
1S_0	-15.6	0.5
3P_2	-1.2	2.5
1G_4	0.0	15.0
1D_2	+4.3	1.0
3F_3	+8.5	2.0
3F_2	+9.3	2.5
3F_4	+13.8	2.5

TABLE II. Calculated satellite energy shifts for Ag $L_{2,3}-M_{4,5}M_{4,5}$ Auger lines with reference to 1G_4 diagram line.

Spectator vacancy	Satellite energy shift (eV)
5s	-9.1
4d	-16.8
4p	-18.8
4s	-12.9
$3d^2$	-5.4
$3d$	-33.4

which has not been identified by Mariot *et al.*,²⁰ appears to arise from the presence of a $3d$ spectator vacancy. This vacancy is produced by the most intense of the L_2-L_3 Coster-Kronig transitions.

Most spectator vacancies are produced by double photoionization through dynamic correlation effects (shake processes).²³ Shake probabilities were calculated in the sudden approximation.²⁴ The results are listed in Table III for shake-off; shake-up probabilities were found to be three to four orders of magnitude smaller, and hence negligible.

D. Error analysis

The data were fitted to Pearson VII functions,²⁵ and a least-squares analysis was applied. The fits include a step function describing a continuous background contribution, the four parameters contained in the Pearson functions, and a similar background function. Photopeaks were used to test the normalization procedure. The variance of calculated intensity over a number of fits was used to derive the quoted error.

The incident-photon-flux measurement is a source of error estimated at $\pm 2\%$ from a comparison over time of photopeak intensities with flux measurements. The angle of the grid is fixed relative to the beam, yet the current from the grid does not reflect fluctuations sensitively in the beam position on the target. The accuracy of the flux measurement is demonstrated in the report by Dikmen.²⁶

III. RESULTS AND DISCUSSION

Typical Ag $L-MM$ Auger spectra are illustrated in Fig. 2 directly as measured, before background subtraction, normalization to constant incident-photon flux, and fitting. Fitted spectra with background subtracted are shown in Figs. 3 and 4, where energies and relative intensities of multiplet components are indicated by bars. An arrow marks the 1G_4 satellite caused by an L_3 spectator

TABLE III. Calculated shake-off probabilities for Ag (in percent).

	3d	4s	4p	4d	5s
2s	1.4	0.3	1.8	14.3	18.4
2p	1.3	0.3	1.9	14.4	18.5

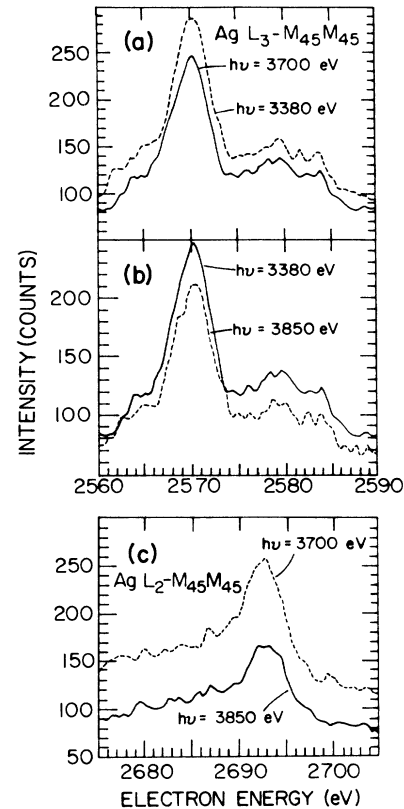


FIG. 2. Typical measured Ag $L_2-M_{4,5}M_{4,5}$ Auger spectra, before background subtraction and fitting.

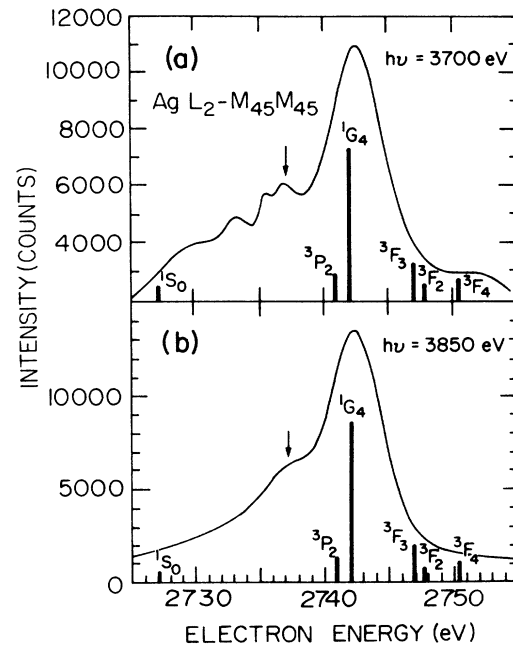


FIG. 3. Fitted Ag $L_2-M_{4,5}M_{4,5}$ Auger spectra excited with x rays of 3700- and 3850-eV energy. Bars indicate multiplet component energies and intensities. (The energy scale includes an 8-eV calibration offset.)

TABLE IV. Measured intensities of Ag L - MM Auger groups excited at various photon energies, normalized to incident photon flux.

Photon energy (eV)	Transition	Relative intensity
3380	L_3 - $M_{4,5}M_{4,5}$	5.06 ± 0.07
3700	L_3 - $M_{4,5}M_{4,5}$	4.42 ± 0.06
3700	L_2 - $M_{4,5}M_{4,5}$	5.06 ± 0.07
3850	L_2 - $M_{4,5}M_{4,5}$	4.53 ± 0.05
3350	L_3 - $M_{4,5}M_{4,5}$	4.36 ± 0.06

vacancy, discussed in Sec. II C. From these spectra, including satellites in the scan region, the relative intensities of the L - MM Auger groups per unit incident-photon flux was determined; results are listed in Table IV. The calculated intensity of satellites with energies below the scan region was included in the final computations as a correction term.

From the relative Auger intensities per unit photon flux measured at three different x-ray energies (Table IV), the L -shell Coster-Kronig transition yields f_{ij} were calculated as described in Sec. II B. The results are listed in Table V, along with theoretical predictions.²⁷ A comparison with theory is of interest because the present results include the first experimental measurement of f_{23} for an atom lighter than Xe,²⁸ the only measurement of f_{12} for an atom with atomic number below $Z=63$,²⁹ and the only determination of f_{13} for an atom in this region of the periodic table but for the recent work on Y by Jitschin *et al.*³⁰

L -shell Coster-Kronig yields have been calculated by McGuire³¹ from exact solutions of the Schrödinger equation in an approximate Herman-Skillman (Hartree-Slater) potential. Crasemann *et al.*³² computed L_1 -shell transition probabilities and fluorescence yields from nonrelativistic screened hydrogenic wave functions. The most recent work on L -shell widths and fluorescence yields is due to Chen *et al.*,²⁷ who calculated relativistic Auger rates from perturbation theory with Dirac-Hartree-Slater wave functions, using the Møller operator.³³ While that calculation includes relativity and quantum electrodynamics (QED), it was performed with frozen orbitals using the independent-particle model, thereby neglecting configuration interaction.

For f_{23} , agreement between the present measurement and the prediction of Ref. 27 is excellent, indicating that the L_2 -hole state in Ag appears to have pronounced

TABLE V. Ag L -shell Coster-Kronig yields f_{ij} from the present work, compared with theoretical predictions.

Coster-Kronig yield	Present measurement	Theory ^a
f_{12}	0.044 ± 0.004	0.068
f_{13}	0.61 ± 0.05	0.740
f_{23}	0.16 ± 0.03	0.155

^aReference 27.

single-particle character and that correlation effects on the L_2 Coster-Kronig yield are relatively small.

The measured $2s$ -subshell yields f_{12} and f_{13} , on the other hand, fall below the independent-particle predictions²⁷ by 35% and 18%, respectively. Discrepancies in the same direction have been observed for the L_1 Coster-Kronig yields of heavier elements,¹⁴ and have long been known to exist for the widths of $2s$ hole states;^{4,8} for example, the Ag $2s$ width of 4.88 eV from the semiempirical fit of Krause and Oliver³⁴ lies 30% below the theoretical width of 6.85 eV from the relativistic independent-particle-model calculation of Chen *et al.*²⁷ In their recent measurement of f_{13} for Y ($Z=39$) by the same method used here, Jitschin *et al.*³⁰ find a result that falls 34% below that of Ref. 27.

The striking disparity of $2s$ -level dynamical properties from the single-particle-model predictions can most likely be ascribed to one or both of the following factors. (i) The calculations are based on Wentzel's ansatz,³⁵ i.e., on the result of time-dependent perturbation theory commonly known as "Fermi's golden rule no. 2." This approach can be expected to fail when there is not a suitably well-defined initial quasistationary state. (ii) The independent-particle model fails when correlations, including interaction with radiationless continua, play a significant role.

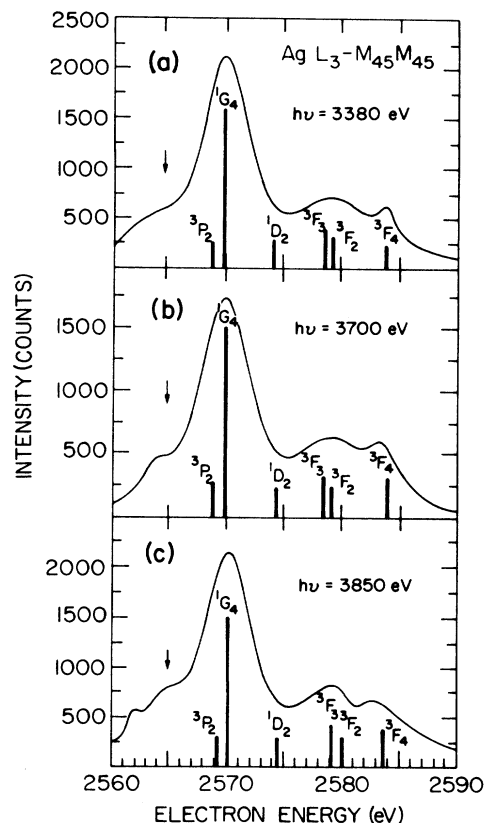


FIG. 4. Fitted Ag L_3 - $M_{4,5}M_{4,5}$ Auger spectra excited with x-rays of 3380-, 3700-, and 3850-eV energy. Bars denote multiplet energies and intensities. (The energy scale includes an 8-eV calibration offset.)

The first factor can be examined crudely by asking how many revolutions the core hole makes during its mean life in a screened hydrogenic model.³⁶ It turns out that the L_1 hole decays on average after some 200 periods and the L_2 hole, after approximately 500 periods, which should be sufficient in both cases to establish the initial state.

The discrepancy between experimental $2s$ Coster-Kronig yields f_{1j} and predictions from the relativistic independent-particle self-consistent-field calculations of Ref. 27 can therefore with considerable certainty be ascribed to the effect of correlations, particularly through dynamic relaxation processes in which the core hole fluctuates to intermediate levels of the Coster-Kronig type, in addition to creating electron-hole pair excitations.^{8,37,38} These effects can be estimated by finite configuration-interaction of multiconfiguration Hartree-Fock methods;^{5,8} when the hole state is embedded in the radiationless continuum, Fano's approach³⁹ of configuration interaction with the continuum is applicable, or the in-

teraction with the Auger continua can be treated by random-phase-approximation methods.⁴⁰ The advent of new experimental data on $2s$ hole-state properties may stimulate further theoretical efforts to treat these perplexing many-body effects.

ACKNOWLEDGMENTS

We gratefully acknowledge the help and advice of Wolfgang Jitschin in planning and executing the initial stages of this experiment. The expert technical assistance of Matt Richter, Mike Rowan, Ann Waldhauer, and Joseph C. Woicik was indispensable. This research was supported in part by National Science Foundation Grant No. PHY-85 16788 and Air Force Office of Scientific Research Grant No. AFOSR-87-0026. The experiment was performed at the Stanford Synchrotron Radiation Laboratory which is funded by the DOE under Contract No. DE-AC03-82ER-13000, Office of Basic Energy Sciences, Division of Chemical Sciences.

- ¹D. Coster and R. de L. Kronig, *Physica* **2**, 13 (1935).
- ²M. H. Chen, B. Crasemann, and H. Mark, *Phys. Rev. A* **27**, 2989 (1983).
- ³W. Bambynek, B. Crasemann, R. W. Fink, H.-U. Freund, H. Mark, C. D. Swift, R. E. Price, and P. Vanugopala Rao, *Rev. Mod. Phys.* **44**, 716 (1972). For an update on yields, see M. O. Krause, *J. Phys. Chem. Ref. Data* **8**, 307 (1979).
- ⁴K. R. Karim, M. H. Chen, and B. Crasemann, *Phys. Rev. A* **29**, 2605 (1984).
- ⁵K. R. Karim and B. Crasemann, *Phys. Rev. A* **31**, 709 (1985).
- ⁶M. H. Chen, B. Crasemann, and H. Mark, *Phys. Rev. A* **24**, 1158 (1981).
- ⁷M. H. Chen, in *Atomic Inner-Shell Physics*, edited by B. Crasemann (Plenum, New York, 1985), Chap. 2.
- ⁸M. H. Chen, B. Crasemann, N. Mårtensson, and B. Johansson, *Phys. Rev. A* **31**, 556 (1985).
- ⁹K. D. Sevier, *Low-Energy Electron Spectrometry* (Wiley-Interscience, New York, 1972).
- ¹⁰L. A. Catz, *Phys. Rev. A* **36**, 3155 (1987).
- ¹¹J. L. Campbell and P. L. McGhee, *J. Phys. (Paris) Colloq.* **48**, C9-597 (1987); P. L. McGhee and J. L. Campbell, *J. Phys. B* **21**, 2295 (1988).
- ¹²W. Jitschin, G. Materlik, U. Werner, and P. Funke, *J. Phys. B* **18**, 1139 (1985).
- ¹³U. Werner and W. Jitschin, *J. Phys. (Paris) Colloq.* **48**, C9-559 (1987).
- ¹⁴U. Werner and W. Jitschin, *Phys. Rev. A* **38**, 4009 (1988).
- ¹⁵J. H. Scofield, Lawrence Livermore Radiation Laboratory Report No. UCRL-51326, 1973 (unpublished).
- ¹⁶J. H. Hubbell and W. J. Veigele, *Comparison of Theoretical and Experimental Photoeffect Data 0.1 keV to 1.5 MeV*, Natl. Bur. Stand. (U.S.) Technical Note No. 901 (U.S. GPO, Washington, D.C., 1976).
- ¹⁷W. Jitschin, U. Werner, G. Materlik, and G. D. Doolen, *Phys. Rev. A* **35**, 5038 (1987).
- ¹⁸Z. Hussain, E. Umbach, D. A. Shirley, J. Stöhr, and J. Feldhaus, *Nucl. Instrum. Methods* **195**, 115 (1982).
- ¹⁹M. J. Berger and J. H. Hubbell, Natl. Bur. Stand. (U.S.) Report No. NBSIR 87-3597, 1987 (unpublished).
- ²⁰J.-M. Mariot, C. F. Hague, and G. Dufour, in *Inner Shell and X-Ray Physics of Atoms and Solids*, edited by D. J. Fabian, H. Kleinpoppen, and L. M. Watson (Plenum, New York, 1981), p. 513; J.-M. Mariot and M. Ohno, *Phys. Rev. B* **34**, 2182 (1986).
- ²¹M. Ohno and G. Wendin, *J. Phys. C* **15**, 1787 (1982).
- ²²C. Froese-Fischer, *Comput. Phys. Commun.* **14**, 145 (1978).
- ²³T. Åberg, *Ann. Acad. Sci. Fenn. Ser. A6*: **308**, 1 (1969).
- ²⁴G. B. Armen, Ph.D. Thesis, University of Oregon, 1985 (unpublished); B. Crasemann, *J. Phys. (Paris) Colloq.* **48**, C9-389 (1987).
- ²⁵K. Pearson, *Biometrika* **16**, 157 (1924).
- ²⁶F. D. Dikmen (unpublished).
- ²⁷M. H. Chen, B. Crasemann, and H. Mark, *Phys. Rev. A* **24**, 177 (1981).
- ²⁸P. B. Semmes, R. A. Braga, J. C. Griffin, and R. W. Fink, *Phys. Rev. C* **35**, 749 (1987).
- ²⁹V. R. Veluri and P. Venugopala Rao, *Z. Phys. A* **280**, 317 (1977).
- ³⁰W. Jitschin, G. Grosse, and P. Röhl, *Phys. Rev. A* **39**, 103 (1989).
- ³¹E. J. McGuire, *Phys. Rev. A* **3**, 587 (1971).
- ³²D. Crasemann, M. H. Chen, and V. O. Kostroun, *Phys. Rev. A* **4**, 2161 (1971).
- ³³M. H. Chen, E. Laiman, B. Crasemann, M. Aoyagi, and H. Mark, *Phys. Rev. A* **19**, 2253 (1979).
- ³⁴M. O. Krause and J. H. Oliver, *J. Phys. Chem. Ref. Data* **8**, 328 (1979).
- ³⁵G. Wentzel, *Z. Phys.* **43**, 524 (1927).
- ³⁶D. Hartree, *The Calculation of Atomic Structures* (Wiley, New York, 1957), Chap. 7.
- ³⁷D. R. Beck and C. A. Nicolaides, in *Excited States in Quantum Chemistry*, edited by C. A. Nicolaides and D. R. Beck (Reidel, Dordrecht, 1978).
- ³⁸M. Ohno and G. Wendin, *J. Phys. B* **11**, 1557 (1979); **12**, 1305 (1979).
- ³⁹U. Fano, *Phys. Rev.* **124**, 1866 (1961).
- ⁴⁰G. Wendin and M. Ohno, *Phys. Scr.* **14**, 148 (1976); **16**, 299 (1977).